ChemPubSoc Europe

DOI: 10.1002/slct.201600027

Chemistry SELECT Full Papers

Materials Science inc. Nanomaterials & Polymers

Rhodamine-Immobilised Electrospun Chitosan Nanofibrous Material as a Fluorescence Turn-On Hg^{2+} Sensor

Nesrin Horzum,[a] Derya Mete,[b] Erman Karakuş,[b] Muhammed Üçüncü,[b] Mustafa Emrullahoğlu,*[b] and Mustafa M. Demir*[c]

A turn-on fluorescence sensing system for mercuric (Hg^{2+}) ions relying on a modified rhodamine B–chitosan fluorophore moiety was developed. This novel sensing approach relies on the simultaneous electrospinning of chitosan and rhodamine B hydrazide with phenylisothiocyanate functionality in hexafluoroisopropanol solution at 3.4 kV cm^{-1}. The electrospun mats exhibited not only considerably enhanced fluorescence intensity in the presence of mercury ions, a result attributed to the ring opening of the spirolactam unit of the rhodamine-based fluorophore, but also a remarkably high sensitivity and selectivity toward Hg^{2+}. In effect, the strategy has the potential to open new avenues in the design and development of other high-performance nanofibrous sensing materials for detecting target metal species of environmental interest.

Introduction

A caustic, carcinogenic element with high cellular toxicity, mercury (Hg) is among the most hazardous pollutants to the environment[1]. The industrial and agricultural use of mercury is a primary source of mercury accumulation[2], whereas mercury pollution originates in nature itself. Oceanic and volcanic eruptions, coal plants, thermometers, caustic soda, gold production, and mercury lamps cause mercury contamination in the air, water, and soil[1a,3]. In humans, the accumulation of mercury causes serious damage to the nervous system, even if its concentration is only in parts per million. The World Health Organization (WHO) has estimated a tolerable concentration of elemental mercury vapour to be 0.2 μg/m^3 for long-term inhalation and a tolerable intake of total mercury to be 2 μg/kg body weight per day[4]. At the same time, the US Environmental Protection Agency (EPA)[5] and US Food and Drug Administration (FDA) have set a limit of 2 parts inorganic mercury per billion in drinking water posing no other lethal adverse health effects[6].

Considerable attention has been paid to the development of new methods for the selective and sensitive detection of mercury species due to their highly toxic nature. Common techniques for detecting mercury ions include inductively coupled plasma mass spectrometry, inductively coupled plasma atomic emission spectrometry, cold vapour atomic absorption spectrometry, neutron activation analysis, X-ray fluorescence spectrometry, atomic fluorescence spectrometry, and spectrophotometry[7]. However, most of these techniques require expensive instruments and time-consuming sample preparations. In response, sensing tools based on instant changes in colour of fluorescence and emission intensity have become quite popular in detecting trace metal ions in various media—for instance, aqueous solutions and living cells. The design of fluorescence-based sensors thus represents a simple, yet sensitive technique for identifying Hg^{2+}.

In this context, the rhodamine framework has emerged as an excellent candidate for constructing off–on fluorescent sensors, given its exceptional photophysical properties such as large molar extinction coefficients and high fluorescence quantum yields. Depending on conditions, the spirocyclic derivatives of rhodamine can exist in two isomeric forms; in the closed isomeric form, the dye is non-fluorescent and colourless, whereas in the open amide form, the dye takes on a characteristic pink colour and emits strong fluorescence. This unique behaviour of rhodamine has been exploited as a signal modulation mechanism in designing a variety of chemosensors.[8]

To improve the overall efficiency of chemosensors in terms of sensitivity, detection limit, and response time, one approach entails assembling the small probe structure on a carrier with adequately small dimensions, including SBA-15, MCM-41, silicon nanowires, silicon nanoparticles, and nanofibres. Among possible carriers, nanofibres with a large surface area per unit mass can enhance the sensitivity of a sensor by interacting with molecules on the surface[9].

At the same time, electrospinning is a facile approach for the versatile fabrication of high surface area sensor interfaces[10]. This process usually offers a large surface-to-volume ratio, controllable morphology, and feasible mechanical strength. Moreover, the internal structure of the electrospun film possesses space (i.e., pores) between nonwoven fibres that allows homogeneous surface treatment[11]. Previously, our team of re-

[a] Dr. N. Horzum
Department of Engineering Sciences
Izmir Katip Celebi University, 35620, Turkey
[b] D. Mete, E. Karakuş, M. Üçüncü, Dr. M. Emrullahoğlu
Department of Chemistry
Izmir Institute of Technology, 35430, Turkey
E-mail: mustafaemrullahoglu@iyte.edu.tr
[c] Prof. M. M. Demir
Department of Materials Science and Engineering
Izmir Institute of Technology, 35430, Turkey
E-mail: mdemir@iyte.edu.tr

Supporting information for this article is available on the WWW under http://dx.doi.org/10.1002/slct.201600027

searchers successfully demonstrated the removal of uranyl ions using the surface treatment with polyacrylonitrile fibres. Nitrile groups were treated with hydroxylamine hydrochloride and underwent amidoximation for selective binding to uranyl groups[12]. Among other applications, electrospun mats have been used in sensors, filters, scaffolds, smart textiles, catalysts, composites, cosmetics, and pharmaceuticals[13].

Recently, nylon-6, poly[1-(4-vinylbenzyl uracil)], poly(vinyl alcohol), and ethyl cellulose nanofibres produced by electrospinning have been used in mercury-sensing applications[14]. Ding et al. developed polyaniline-based nanofibres as a sensor for the colorimetric detection of Hg^{2+} ions that showed good reversibility after extended regeneration cycles[15]. Another efficient strategy for detecting Hg^{2+} ions was reported by Cai et al.[16] for the in situ preparation of fluorescent gold nanoclusters with an electrospun bovine serum albumin–poly(ethylene oxide) mat.

Given its biocompatibility, biodegradability, and non-toxicity as a natural biopolymer, the (1→4)-2-amino-2-deoxy-β-D-glucan chitosan has been the focus of many investigations. Interestingly, chitosan is an N-deacetylated product of chitin, the second most abundant natural polysaccharide after cellulose[17]. Chitosan has also been used as a substrate for the covalent immobilisation of target molecules given its abundant amine and hydroxyl functional groups[18].

In this study, we designed novel flexible, turn-on electrospun nanofibres with the modified rhodamine B (**Md-RhB**)–chitosan fluorophore moiety for detecting Hg^{2+}. A major advantage of this method is that the highly specific surface area of the nanofibres provides a high number of functional groups per gram of substrate. Furthermore, compared with powdered materials, nanofibrous mats have mechanical integrity, which makes them easy to handle. The electrospun mats also exhibit high selectivity and excellent sensitivity to Hg^{2+}, to as little as 10^{-9} mM.

Results and Discussion

Rhodamine conjugate was obtained from the reaction of an electrophilic *p*-phenylene diisothiocyanate and nucleophilic RhB hydrazide, whereas chitosan-based nanofibres loaded with **Md-RhB** were obtained by electrospinning using 1,1,1,3,3,3-hexafluoro-2-propanol (HFIP) as the solvent. Figure 1 shows a flowchart of the preparation of **Md-RhB–chitosan** fibres.

HFIP plays a critical role in biopolymer dissolution, given its exceptionally strong hydrogen bond donor, which breaks hydrophobic interactions, and its high acidity (pK_a 9.3), which breaks hydrogen bonding[19]. It is worth mentioning that the acidic nature of the solvent causes a ring-opening reaction of the spirolactam ring and becomes a highly fluorescent rhodamine derivative. Depending on the solution's pH level, the structure exhibits a reversible ring opening (fluorescence 'ON') and closuring (fluorescence 'OFF') process. **Md-RhB–chitosan** nanofibres were thus treated with a triethylamine (TEA) solution to obtain the non-fluorescent form. The prepared TEA solution used in treating **Md-RhB–chitosan** nanofibres was used as a fluorescent probe for detecting Hg^{2+}.

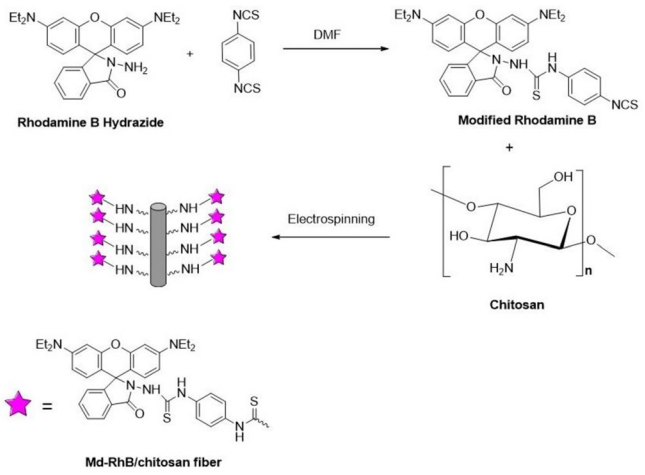

Figure 1. Synthetic route for the preparation of **Md-RhB/chitosan fibres**.

The literature includes many examples of fluorescent probes based on the high affinity of mercury ions toward sulphur-containing groups. Given this knowledge, our investigation commenced by screening the response of **Md-RhB–chitosan** nanofibres to mercury ions. As expected, the **Md-RhB–chitosan** nanofibres induced a rapid turn-on response to mercury ions.

One of the most important features for constructing a favourable fluorescent sensor is its selectivity to a target metal ion. In this regard, the selectivity profile of **Md-RhB–chitosan** nanofibres to Hg^{2+} was investigated over a range of potentially competing ions, including alkaline earth, heavy, and transition metal ions (Ni^{2+}, Pd^{2+}, Zn^{2+}, Mg^{2+}, Pb^{2+}, Fe^{2+}, Cu^{2+}, Co^{2+}, Cr^{2+}, and Cd^{2+}), all using confocal microscopy (Figure 2).

The cations employed did not prompt any significant changes in fluorescence, even when treated with 20 mM concentrations of the respective metal ions. However, only the addition of Hg^{2+} enhanced the fluorescence, entirely as a result of the Hg^{2+}-induced ring opening of the spirolactam form when excited under 525 nm[20].

For further insights into whether the sensing mechanism is reversible, we added sodium sulphide to the sensing system pretreated with mercury ions. Neither a change in colour nor in emissions of **Md-RhB–chitosan** nanofibres was observed. It was thus proven that the sensing event occurred in an irreversible way. The proposed reaction mechanism of **Md-RhB–chitosan** nanofibres with Hg^{2+} appears in Figure 3. Hg^{2+} ions exhibited a high affinity to sulphur atoms in the thiosemicarbazide group and underwent an irreversible desulphurisation–cyclisation reaction to form a 1,3,4-oxadiazole derivative as a new spacer and, in turn, a fluorescent product[21].

To further clarify the chemistry of the binding process, a model probe system, **Md-RhB-Bn**, was constructed by reacting **Md–Md-RhB** with a representative aliphatic amine (e.g benzylamine ($BnNH_2$)). The binding process of Hg^{2+} to **RhB-Bn** was followed by the aid of ^{1}H-NMR spectroscopy. Figure 4 displays the ^{1}H-NMR spectra of **Md-RhB**, **Md-RhB-Bn** and the cyclization product of the probe **Md-RhB-Ox.** Pronounced differences in

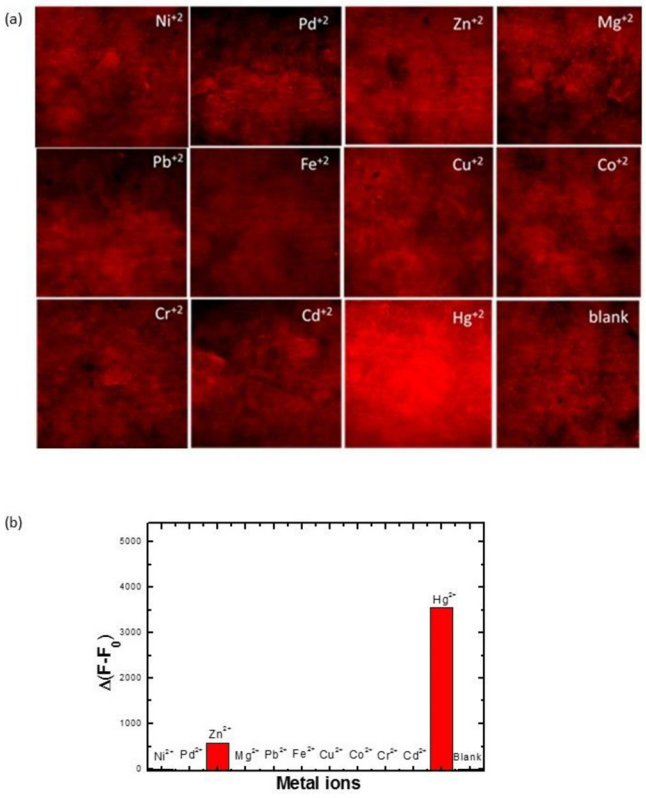

Figure 2. a) Confocal microscopy images of TEA treated **Md-RhB/chitosan** nanofibres, b) Relative fluorescence intensity of the nanofibres after different metal solutions (20 mM) treatment..

Figure 3. Schematic representation of the cyclization reaction of TEA treated Md-RhB/chitosan nanofibres.

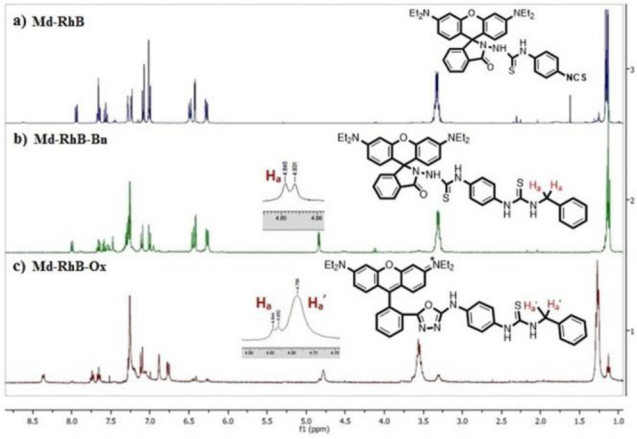

Figure 4. ^{1}H NMR spectra of model system a) **Md-RhB** b) **Md-RhB-Bn** c) **Md-RhB-Ox** (treated with 1 equiv. Hg^{2+}) in $CDCl_3$.

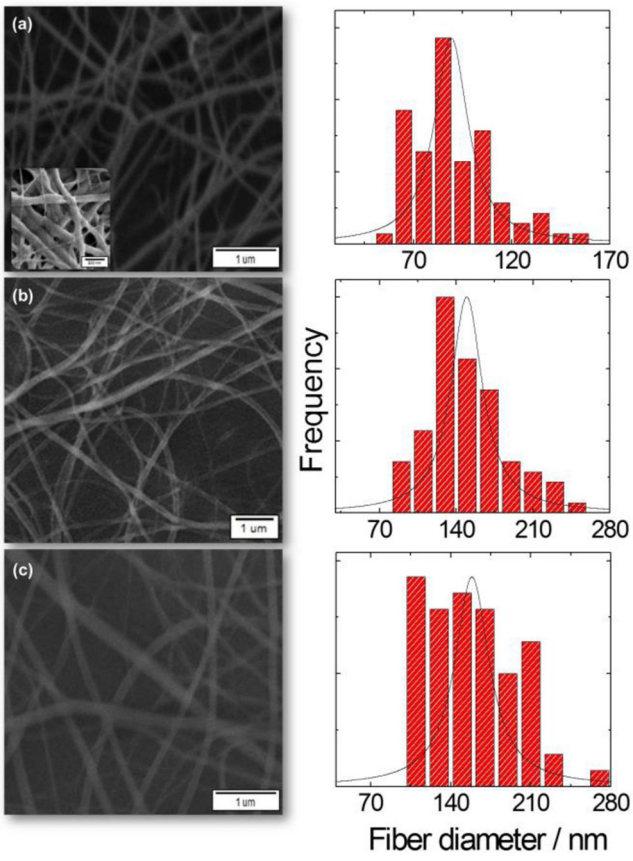

Figure 5. SEM micrographs of the a) Md-RhB/chitosan fibre b) **Md-RhB/chitosan** fibre after TEA treatment, and c) TEA treated **Md-RhB/chitosan** fibre after addition of Hg^{2+} solution..

the ^{1}H-NMR spectrum of **Md-RhB-Bn** were monitored during the incubation of Hg^{2+}. For one, the resonance of the benzylic proton signal (H_a) at 8.01 ppm was slightly shifted to a lower frequency, while the resonance of the diethylamine-CH_2 proton signals at 3.3 ppm shifted to a higher frequency (e.g. 3.6 ppm). Furthermore, the resonances of aryl ring protons (e.g. 6.2-6.5 ppm and 8.1 ppm) dramatically shifted to higher frequencies (see Supporting Information) strongly suggesting a structural modification from ring-closed to ring-opened form of the probe structure in consistent with literature data.[21–22]

The SEM micrographs of **Md-RhB–chitosan** fibres in Figure 5 illustrate the evolution of the surface structures after the surface treatment of the fibres and their exposure to aqueous Hg^{2+} solution. The **Md-RhB–chitosan** fibres exhibited a smooth, continuous, and uniform surface, with an average diameter of 95 ± 20 nm (Figure 5a). The morphologies obtained after the base treatment or the addition of Hg^{2+} solution (Figure 5b–c) posed no serious deterioration or breakage of the fibres. Upon posttreatment, an increase in the fibre mean diameter by roughly 60% was observed. Moreover, the fibre diameter

distribution widened, and the average fibre diameter for the TEA-treated and of the fibre after adding Hg^{2+} increased to 150 ± 35 and 160 ± 40 nm, respectively. Nevertheless, the integrity of the fibres was preserved.

Figure 6 shows the FTIR spectra of the fibres. The spectrum of chitosan contains broad -OH stretching absorption bands

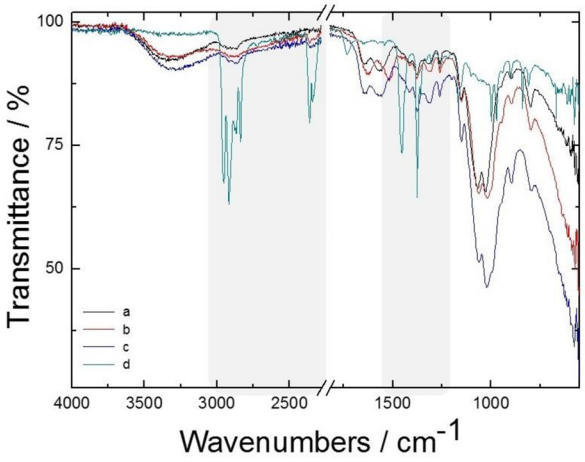

Figure 6. FTIR spectra of the electrospun nanofibres a) chitosan, b) **Md-RhB/chitosan**, c) TEA treated **Md-RhB/chitosan**, d) TEA treated **Md-RhB/chitosan** after addition of Hg^{2+} solution.

between 3600–3300 cm^{-1}. The absorption band between 3000–2800 cm^{-1} is assigned to aliphatic C–H stretching. The spectrum within the range of 1280–1230 cm^{-1} is attributed to the stretching vibrations of C–O groups. A characteristic free primary amino group (-NH_2) at the C2 position of glucosamine present in the chitosan is identified within the spectral range of 1200–1000 cm^{-1}. A series of new characteristic bands emerged for the **Md-RhB–chitosan** fibre at around 1628 cm^{-1}, 1518 cm^{-1}, and 1150 cm^{-1} are attributed to stretching vibrations of C=O, C=C, and C=S, respectively. For TEA treated **Md-RhB–chitosan** fibre, the intensity of the absorption bands associated with C–H and C–N streching increases. After adding the Hg^{2+} solution, the ring-opening of the spirolactam and a ring-opened amide caused the formation of new absorption bands[23]. The aromatic C–H stretch yielded broad, intense absorption band between 3000–2800 cm^{-1}, and a ring consisting of isocyanate appears at roughly 2350 cm^{-1}. The band related with the bending of N–H was also centred at 1446 cm^{-1}, and the sharp signal at 1337 cm^{-1} could be referred to as C–N stretching in aromatic amines. Upon addition of Hg^{2+} solution, the signal of the carbonyl group disappeared due to the formation of 1,3,4-oxadiazole ring.

A distinct change in fluorescence emission from colourless to red–pink under 366 nm UV light obtained for the TEA-treated **Md-RhB–chitosan** nanofibres in the presence of Hg^{2+} appears in Figure 7. The nanofibre probe showed a 'turn-on' fluorescent response when reacting with Hg^{2+}, thus inducing the ring-opening of the spirolactam followed by cyclisation.

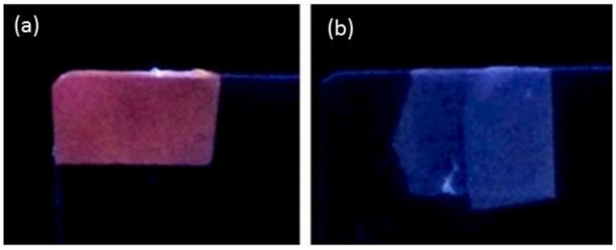

Figure 7. Photographic images of the electrospun nanofibres a) TEA treated **Md-RhB/chitosan** after Hg^{2+} addition, b) TEA treated **Md-RhB/chitosan** under UV light.

Md–RhB-loaded electrospun nanofibres demonstrated a response over the concentration range of 1.0 × 10^{-7} to 20 mM for Hg^{2+} ions. Figure 8 shows the fluorescence microscopy images of the nanofibres and the nanofibres' fluorescence intensity concentration in the range of 20–2 × 10^{-4} mM. Upon increasing the concentration of Hg^{2+}, fluorescence intensity improved. Fluorescence microscopy experiments demonstrated that the **Md-RhB–chitosan** nanofibres can be used to detect Hg^{2+} ions, even at 10^{-9} mM.

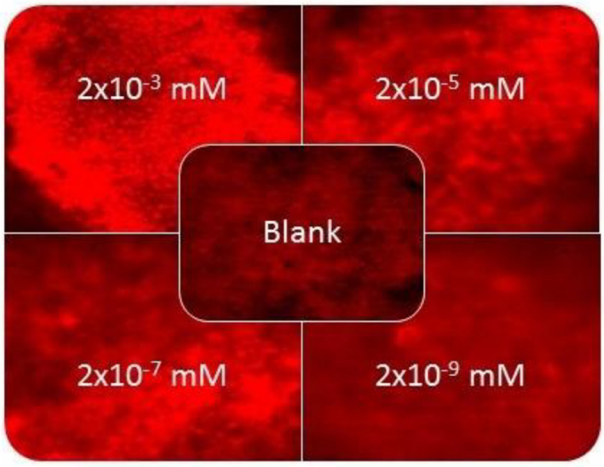

Figure 8. Fluorescence microscopy images of TEA treated **Md-RhB/chitosan** nanofibres after addition of different Hg^{2+} ion concentrations.

Conclusions

Highly fluorescent and flexible Md-RhB–chitosan nanofibres were designed and obtained by electrospinning. The developed spirocyclic RhB derivative grafted chitosan nanofibres used as a fluorescence turn-on probe, which allowed the selective detection of Hg^{2+} ions by the opening of the spirolactam ring of the rhodamine unit. The useful feature of the highly specific surface area in terms of number of available functional groups per gram on the freestanding mat enhanced the sensitivity of the Hg^{2+}-sensing probe. The strategy thereby

eliminates the need for centrifugation and filtration, thus providing practicality in the environmental monitoring of toxic mercury. The response of the Hg^{2+}-selective nanofibre mat was examined by both colorimetric changes and changes in fluorescence intensity. These findings show that the rapid determination of Hg^{2+} ions can be expanded to other functional nanomaterials for the detection of undesirable metal ions in the environmental field.

Supporting Information

The detailed Experimental Section involving ^{1}H and ^{13}C NMR spectra of **Md-RhB** and **Md-RhB-Bn**, ^{1}H NMR spectra of the model system, absorbance and fluorescence spectra, and reaction time profiles of **Md-RhB-Bn**, has been provided in Supporting Information.

Acknowledgements

The authors acknowledge Aidyn Pidahmet for his contribution to the initial stage of the experiments, the Center of Material Research and Biotechnology Research and Application Center, Environmental Research Center of Izmir Institute of Technology.

Keywords: Chitosan · fluorescence imaging · mercury sensing · nanofibre · rhodamine

[1] a) A. Carocci, N. Rovito, M. S. Sinicropi, G. Genchi, *Rev. Environ. Contam. Toxicol.* **2014**, *229*, 1–18; b) J. S. Lee, M. S. Han, C. A. Mirkin, *Angew. Chem.* **2007**, *119*, 4171–4174 ; Angew. Chem. Int. Ed. Engl. **2007,** 46, 4093–4096.

[2] P. C. Nagajyoti, K. D. Lee, T. V. M. Sreekanth, *Environ. Chem. Lett.* **2010**, *8*, 199–216.

[3] a) F. Di Natale, A. Lancia, A. Molino, M. Di Natale, D. Karatza, D. Musmarra, *J. Hazard. Mater.* **2006**, *132*, 220–225; b) A. B. Mukherjee, R. Zevenhoven, P. Bhattacharya, K. S. Sajwand, R. Kikuchi, *Resour., Conserv. Recyc.* **2008**, *52*, 571–591.

[4] *Bull. W. H. O.* **2013**, *91*, 161–162.

[5] J. Johnson, *Environ. Sci.Technol.* **1997**, *31*, 218 A-219 A.

[6] C. Diez-Gil, R. Martinez, I. Ratera, T. Hirsh, A. Espinosa, A. Tarraga, P. Molina, O. S. Wolfbeis, J. Veciana, *Chem. Commun.* **2011**, *47*, 1842–1844.

[7] a) W. L. Clevenger, B. W. Smith, J. D. Winefordner, *Crit. Rev. Anal. Chem.* **1997**, *27*, 1–26; b) M. J. Powell, E. S. K. Quan, D. W. Boomer, D. R. Wiederin, *Anal. Chem.* **1992**, *64*, 2253–2257; c) M. Guerrero, J.-L. Todolí, J. Mora, A. Canals, *Anal. Lett.* **1999**, *32*, 771–785; d) M. Ghaedi, M. Reza Fathi, A. Shokrollahi, F. Shajarat, *Anal. Lett.* **2006**, *39*, 1171–1185; e) P. J. Potts, P. C. Webb, O. Williams-Thorpe, R. Kilworth, *Analyst* **1995**, *120*, 1273–1278; f) C. Zheng, Y. Li, Y. He, Q. Ma, X. Hou, *J. Anal. At. Spectrom.* **2005**, *20*, 746–750.

[8] a) A. Bianchi, E. Delgado-Pinar, E. Garcia-Espana, C. Giorgi, F. Pina, *Coord. Chem. Rev.* **2014**, *260*, 156–215; b) Y. Egawa, T. Seki, S. Takahashi, J. Anzai, *Mater. Sci. Eng. C* **2011**, *31*, 1257–1264; c) M. Dong, T. H. Ma, A. J. Zhang, Y. M. Dong, Y. W. Wang, Y. Peng, *Dyes Pigm.* **2010**, *87*, 164–172.

[9] a) Q. Meng, X. Zhang, C. He, G. He, P. Zhou, C. Duan, *Adv.Funct. Mater.* **2010**, *20*, 1903–1909; b) M. Hosseini, V. K. Gupta, M. R. Ganjali, Z. Rafiei-Sarmazdeh, F. Faridbod, H. Goldooz, A. R. Badiei, P. Norouzi, *Anal. Chim. Acta* **2012**, *715*, 80–85; c) L. Mu, W. Shi, G. She, J. C. Chang, S.-T. Lee, *Angew. Chem.* **2009**, *121*, 3521–3524; *Angew. Chem. Int. Ed. Engl.* **2009**, *48,* 3469–3472*;* d) Z. P. Dong, X. Tian, Y. Z. Chen, Y. P. Guo, J. T. Ma, *RSC Adv.* **2013**, *3*, 1082–1088; e) X. Wang, C. Drew, S.-H. Lee, K. J. Senecal, J. Kumar, L. A. Samuelson, *Nano Lett.* **2002**, *2*, 1273–1275.

[10] a) A. Greiner, J. H. Wendorff, *Angew. Chem.* **2007**, *119,* 5770–5805; *Angew. Chem. Int. Ed. Engl.* **2007**, *46*, 5670–5703; b) Z.-M. Huang, Y.-Z. Zhang, M. Kotaki, S. Ramakrishna, *Compos. Sci.Technol.* **2003**, *63*, 2223–2253.

[11] a) S. Agarwal, J. H. Wendorff, A. Greiner, *Macromol. Rapid Commun.* **2010**, *31*, 1317–1331; b) M. M. Demir, G. Ugur, M. A. Gulgun, Y. Z. Menceloglu, *Macromol. Chem. Phys.* **2008**, *209*, 508–515.

[12] N. Horzum, T. Shahwan, O. Parlak, M. M. Demir, *Chem. Eng. J.* **2012**, *213*, 41–49.

[13] a) L. T. H. Nguyen, S. Chen, N. K. Elumalai, M. P. Prabhakaran, Y. Zong, C. Vijila, S. I. Allakhverdiev, S. Ramakrishna, *Macromol. Mater. Eng.* **2013**, *298*, 822–867; b) P. Gibson, H. Schreuder-Gibson, D. Rivin, *Colloids Surf. A.* **2001**, *187–188*, 469–481.

[14] a) A. Ghosh, V. Jeseentharani, M. A. Ganayee, R. G. Hemalatha, K. Chaudhari, C. Vijayan, T. Pradeep, *Anal. Chem.* **2014**, *86*, 10996–11001; b) Y. S. Wang, C. C. Cheng, J. K. Chen, F. H. Ko, F. C. Chang, *J. Mater. Chem. A* **2013**, *1*, 7745–7750; c) A. Senthamizhan, A. Celebioglu, T. Uyar, *Journal of Mater. Chem. A* **2014**, *2*, 12717–12723; d) S. Kacmaz, K. Ertekin, A. Suslu, Y. Ergun, E. Celik, U. Cocen, *Mater. Chem. Phys.* **2012**, *133*, 547–552.

[15] Y. Si, X. Q. Wang, Y. Li, K. Chen, J. Q. Wang, J. Y. Yu, H. J. Wang, B. Ding, *J. Mater. Chem. A* **2014**, *2*, 645–652.

[16] Y. Q. Cai, L. Yan, G. Y. Liu, H. Y. Yuan, D. Xiao, *Biosens. Bioelectron.* **2013**, *41*, 875–879.

[17] M. N. V. Ravi Kumar, *React. Funct. Polym.* **2000**, *46*, 1–27.

[18] W. S. Wan Ngah, C. S. Endud, R. Mayanar, *React. Funct. Polym.* **2002**, *50*, 181–190.

[19] a) A. Berkessel, J. A. Adrio, D. Hüttenhain, J. M. Neudörfl, *J. Am. Chem. Soc.* **2006**, *128*, 8421–8426; b) L. Eberson, M. P. Hartshorn, O. Persson, F. Radner, *Chem. Commun.* **1996**, 2105–2112.

[20] a) H. N. Kim, M. H. Lee, H. J. Kim, J. S. Kim, J. Yoon, *Chem. Soc. Rev.* **2008**, *37*, 1465–1472; b) J.-S. Wu, I.-C. Hwang, K. S. Kim, J. S. Kim, *Org. Lett.* **2007**, *9*, 907–910.

[21] Y. K. Yang, K. J. Yook, J. Tae, *J. Am. Chem. Soc.* **2005**, *127*, 16760–16761.

[22] a) M. Wang, J. Wen, Z. Qin, H. Wang, *Dyes Pigm.* **2015**, *120*, 208–212; b) L. Yuan, W. Y. Lin, Y. N. Xie, B. Chen, J. Z. Song, *Chem. - Eur. J.* **2012**, *18*, 2700–2706; c) X. L. Zhang, Y. Xiao, X. H. Qian, *Angew. Chem.* **2008**, *120,* 8145–8149; *Angew. Chem. Int. Ed. Engl.* **2008**, *47*, 8025–8029.

[23] a) M. H. Lee, J.-S. Wu, J. W. Lee, J. H. Jung, J. S. Kim, *Org. Lett.* **2007**, *9*, 2501–2504; b) M. Pandurangappa, K. S. Kumar, *Anal. Methods* **2011**, *3*, 715–723.

Submitted: January 15, 2016
Accepted: March 31, 2016

FULL PAPERS

Highly fluorescent and flexible Md-RhB–chitosan nanofibres were designed and obtained by the simultaneous electrospinning of chitosan and rhodamine B hydrazide with phenylisothiocyanate functionality for the selective detection of Hg^{2+} ions.

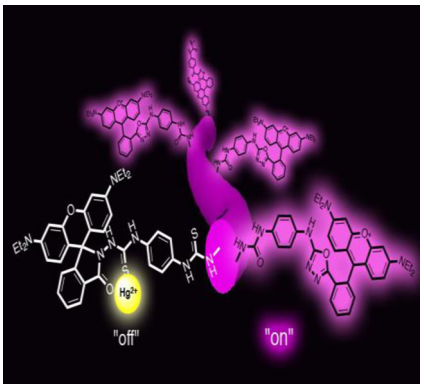

Dr. N. Horzum, D. Mete, E. Karakuş, M. Üçüncü, Dr. M. Emrullahoğlu, Prof. M. M. Demir**